

Femtosecond Time-Resolved Photoelectron Angular Distributions Probed during Photodissociation of NO₂

J. A. Davies,* R. E. Continetti,* D. W. Chandler, and C. C. Hayden†

Combustion Research Facility, Sandia National Laboratories, P.O. Box 969, Livermore, California 94551-0969

(Received 27 January 2000)

Femtosecond time-resolved photoelectron angular distributions (PADs) are measured for the first time in the molecular frame of a dissociating molecule. Various stages of the dissociation process, NO₂ → NO(C²Π) + O(³P), are probed using ionization of the NO(C²Π) fragment to NO⁺(X¹Σ⁺). The PADs evolve from forward-backward asymmetric with respect to the dissociation axis at short time delays (≤500 fs) to symmetric at long time delays (≥1 ps). Changes in the PADs directly reflect the time-dependent separation and reorientation of the dissociating photofragments.

PACS numbers: 33.80.Eh, 33.80.Gj, 33.80.Rv

Measurements of photoelectron angular distributions (PADs) can provide a wealth of information on the nature of the molecular orbital that is ionized, the geometry and orientation of the molecule as the electron departs, and the dynamics of the photoionization process. Unfortunately, much of this information is lost when the PAD is measured from a randomly oriented sample of molecules. As a result, methods have been developed to measure PADs relative to the framework of the molecule. Recently, measurements of these molecular frame PADs have been used to probe shape resonances [1], inner shell ionization [2], valence shell ionization [3,4], and double ionization [5]. Theoretical studies [6–8] have shown that changes in PADs as a function of time, using femtosecond pump-probe ionization, can provide a sensitive probe of molecular motions and orientations. In this paper, we present the first measurements of femtosecond time-resolved PADs in the molecular frame of a dissociating molecule. The changes observed in the PADs during the course of the dissociation directly reflect the time-dependent separation and reorientation of the fragments.

Laboratory frame PADs are usually measured as a function of the angle, θ' , between the electron recoil direction and the electric vector of linearly polarized light. For a randomly oriented gaseous molecular sample under these conditions, the photoionization differential cross section is represented by

$$\frac{d\sigma}{d\Omega'} = \frac{\sigma}{4\pi} [1 + \beta P_2(\cos\theta')], \quad (1)$$

where σ is the integrated cross section, β is the asymmetry parameter, and $P_2(\cos\theta')$ is the second order Legendre polynomial. More detailed information on ionization dynamics is obtained by measuring the PADs with respect to the molecular z axis, rather than averaging over all molecular orientations. For the special case in which the laser polarization is parallel to the z axis of a cylindrically symmetric molecule, the molecular frame PADs are azimuthally isotropic and the differential cross

section is given by [9]

$$\frac{d\sigma}{dk_e} = \sum_{K=0}^{2l_{\max}} A_K P_K(\cos\theta), \quad (2)$$

where $k_e(\theta, \phi)$ is the electron ejection direction in the molecular frame, l_{\max} is the maximum angular momentum of the ejected electron, and $P_K(\cos\theta)$ is the Legendre polynomial of K th order. The expansion coefficients, A_K , provide information on partial wave transition amplitudes and phase shifts that are unobtainable by conventional laboratory frame measurements.

Previous experimental work has employed several different approaches to measure PADs referenced to axes of molecular alignment or orientation. In such experiments, the molecules being ionized exhibit either angular momentum alignment [10], where an axis about which the molecule rotates (rather than a molecular axis) is aligned, or molecular frame orientation [1–4] in which the molecular axis is determined and inversion symmetry along this axis may be broken. The most commonly used technique to obtain molecular frame PADs involves the ionization of a randomly oriented molecular sample to a highly excited state that rapidly dissociates. The fragment ion is detected in coincidence with the electron, such that the molecular orientation of the parent can be determined from the recoil direction of the fragment ion. This technique does not create an oriented molecular sample, but instead determines the orientation of the parent after the fact, one molecule at a time. In the present work, a new variation of this technique is used to study time-resolved ionization of a dissociating molecule. First, a femtosecond pump laser pulse initiates the dissociation of NO₂ and then a time-delayed probe pulse ionizes the incipient NO fragment. The orientation of the dissociation axis is determined from the ion recoil direction, since the dissociation is fast compared to the rotational period of the cold parent molecule. In this way, femtosecond time-resolved PADs are measured in the molecular frame of the dissociating molecule.

For our femtosecond, energy- and angle-resolved photoelectron-photoion coincidence experiments [11], a

regeneratively amplified titanium sapphire laser system is operated at 2.2 kHz producing linearly polarized pulses of 100 fs duration. The pulses are frequency doubled to a peak wavelength of 375.3 nm and split into a pump pulse and a time-delayed probe pulse. The laser beam is focused to an intensity of approximately 10^{12} W cm $^{-2}$ inside an ultrahigh vacuum chamber where it intersects a continuous molecular beam (2% NO $_2$ in Ar). Under these conditions, the pump laser pulse three-photon excites the NO $_2$ to a dissociative state that correlates to NO($C^2\Pi$) + O(3P) [11]. After a variable time delay, the probe laser pulse single photon ionizes NO($C^2\Pi$) to NO $^+$ ($X^1\Sigma^+$). After an ionization event, the electron is gently extracted towards a time- and position-sensitive detector [12]. Following a short time delay (300 ns), the coincident ion is extracted in the opposite direction from the electron and accelerated towards a second time- and position-sensitive detector. The acceptance solid angle for both detectors is 4π , such that full three-dimensional angular distributions are measured. In order to avoid false coincidences, a low ionization rate (1 event per 100 laser shots) is used and ionization events are recorded only if a single ion and a single electron are detected after a laser shot. Over 2×10^6 pairs of coincident ions and electrons are recorded for each pump-probe time delay. Background signal due to the individual pump or probe pulses is subtracted from the time-delayed data.

The initial recoil velocity vectors for the coincident ions and electrons are calculated from their measured arrival times and positions at the detectors. For each ionization event, we determine the angle between the electric vector of the light and the fragment ion velocity vector, and the angle between the fragment ion and coincident electron velocity vectors. Only events in which the ion recoil direction is parallel ($\pm 10^\circ$) to the pump and probe laser polarizations are considered in this paper. Therefore, the resulting three-dimensional electron angular distributions are azimuthally isotropic about the ion recoil axis. In Fig. 1, the PADs are displayed as polar plots of the electron intensity (per unit solid angle) as a function of the angle between the ion and electron recoil directions. The earliest stages of the dissociation are probed with zero pump-probe time delay. In this case, the dissociation and ionization both occur within the duration of a single laser pulse (100 fs). Pump-probe time delays of 350 fs, 500 fs, 1 ps, and 10 ps probe progressively later stages of the dissociation. The experimental PAD for zero time delay [Fig. 1(a)] is strongly forward-backward asymmetric with higher intensity in the direction of NO $^+$ recoil. A prominent lobe is observed at about 30° from the ion recoil direction. As the pump-probe time delay is increased to 350 fs and then to 500 fs [Figs. 1(b) and 1(c), respectively], the asymmetry decreases and the lobe becomes less prominent. At time delays of 1 and 10 ps [Figs. 1(d) and 1(e), respectively], the PADs are symmetric and the lobe at 30° is absent.

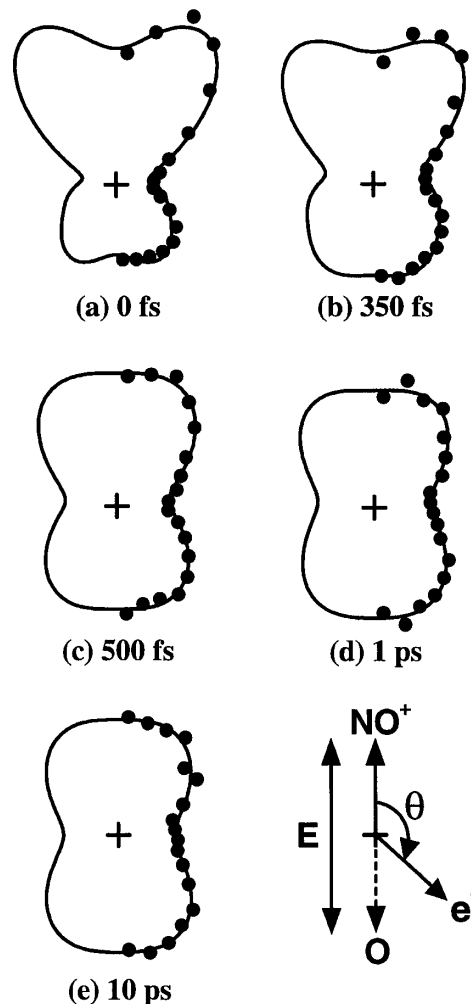


FIG. 1. Photoelectron angular distributions for pump-probe time delays of (a) 0 fs, (b) 350 fs, (c) 500 fs, (d) 1 ps, and (e) 10 ps. The electron intensity (measured in counts per unit solid angle) is represented by the distance between the experimental data points (\bullet) and the origin of the polar plot ($+$) and is plotted as a function of angle, θ , between the ion (NO $^+$) and electron (e^-) recoil directions. Fits ($—$) to the experimental data are calculated using a linear expansion of Legendre polynomials. The electric vectors for the pump and probe laser polarizations (E) are parallel to the ion recoil direction and dissociation axis.

In these experiments, the PADs are measured with respect to the dissociation axis, which is determined by the ion recoil direction. For a cylindrically symmetric molecule, the dissociation axis would also correspond to the z axis of the parent molecule, and the differential cross section would be described by Eq. (2). The geometry of the NO $_2$ dissociative state accessed in these experiments is not known. It is expected to be approximately linear, however, since the product NO(C) rotational state distribution peaks at a low energy [11]. In this work, we have not assumed the geometry of the parent molecule, but have chosen experimental conditions such that the PADs are azimuthally isotropic and can therefore be described by a linear

expansion of Legendre polynomials similar to Eq. (2). Instead of fixing an upper limit of $2l_{\max}$ on the number of expansion terms, we used the minimum number of terms required for a good fit to the experimental data. The empirical fit coefficients, A_K , can be determined regardless of the molecular geometry. In the special case of a cylindrically symmetric molecule with its z axis parallel to the electric vector of the laser polarization, the fit coefficients can be used to calculate partial wave transition amplitudes and phase shifts [1].

The experimental data were fitted to a linear combination of zero to sixth order Legendre polynomials, $d\sigma/d\Omega = \sum A_K P_K(\cos\theta)$ for $K = 0$ to 6. Figure 1 shows excellent agreement between the calculated fit and experimental data for each time delay. The calculated values for the fit coefficients, A_K , are normalized such that $A_0 = 1$ and the results are presented in Table I. The fit coefficients for odd K determine the degree of forward-backward asymmetry, while higher order coefficients are required to describe the lobed feature at 30° from the dissociation axis. Several obvious trends are observed in the magnitudes of the normalized fit coefficients, A'_K , as the pump-probe time delay increases. The odd fit coefficients are observed to approach zero and the magnitudes of higher order even coefficients, A'_6 and A'_4 , rapidly decrease as the time delay increases. Only A'_2 and A'_0 have large contributions at longer time delays of 1 and 10 ps.

In a zero time delay experiment, three-photon excited NO_2 is starting to dissociate, such that the O-NO bond is elongated, when the molecule is single-photon ionized within the 100 fs duration of the excitation laser pulse. The incipient NO fragment is oriented because it has not had time to rotate significantly prior to ionization [a rotational period of at least 1 ps is estimated from the peak of the $\text{NO}(C)$ rotational energy distribution measured after dissociation is complete [11]]. There are two possible effects that could contribute to the forward-backward asymmetry and the lobe at 30° from the dissociation axis observed in the zero time delay PAD [Fig. 1(a)]. First we will consider whether the observed PAD primarily reflects the molecular frame PAD for oriented $\text{NO}(C)$ from the dissociation, in which case the recoiling O atom simply provides a frame of reference for the orientation. On the other hand, if the recoiling O atom strongly influences the ionization of the incipient $\text{NO}(C)$, then this effect of the O atom could be responsible for the observed PAD features.

The first possible cause of the zero time delay PAD features is the ionization of oriented $\text{NO}(C)$ that is relatively unaffected by the close proximity of the O-atom partner. Strongly asymmetric PADs from valence shell ionization of oriented diatomics have previously been calculated by Davenport [13] and are a result of interference between odd and even partial waves due to scattering from the ion core. The molecular frame PAD for $\text{NO}(C)$ has not been reported. However, previous calculations [14] of the electron partial wave composition for ionization of $\text{NO}(C)$ ($3p\pi$ Rydberg state) predict that s and d waves ($l = 0$ and 2, respectively) strongly dominate due to the atomic-like character of the ionization process, with only 1% originating from odd partial waves. This calculation suggests that the molecular frame PAD for free $\text{NO}(C)$ is approximately symmetric and is not responsible for the degree of asymmetry observed in Fig. 1(a). The shape of the lobed feature at 30° from the dissociation axis could result from ionization of free NO fragments that are oriented at an angle relative to the dissociation axis, corresponding to a bent geometry of NO_2 . However, the excited state NO_2 is expected to be approximately linear such that $\text{NO}(C)$ is oriented along the dissociation axis. For linear NO_2 , the fit coefficients in Table I provide information on the electron partial wave composition. The lobe at 30° requires a large f wave ($l = 3$) contribution (indicated by $|A'_6|$), but this result is inconsistent with the strongly dominant s and d waves predicted for free $\text{NO}(C)$ [14]. Based on these arguments, ionization of free, oriented $\text{NO}(C)$ does not simultaneously explain both the asymmetry and lobed feature at 30° observed in the zero time delay PAD.

The most consistent explanation for the zero time delay PAD features is that they result from the effect of the nearby O atom on the ionization of the $\text{NO}(C)$ before the photofragments have separated substantially. Our previous energy analysis of zero time delay experiments [11] shows a broad photoelectron energy distribution that is due to ionization of the incipient $\text{NO}(C)$ in dissociating NO_2 rather than ionization of free $\text{NO}(C)$. Thus, the presence of the O-atom fragment in dissociating NO_2 strongly affects the photoelectron energies and, consequently, is also expected to affect the angular distribution of the photoelectrons. The potential energy surface for the departing photoelectron is highly nonspherical with strong inversion asymmetry due to the neutral O atom starting to recoil from the NO^+ .

TABLE I. Normalized Legendre polynomial fit coefficients, A'_K , for pump-probe time delays up to 10 ps.

| Time delay (fs) | A'_0 | A'_1 | A'_2 | A'_3 | A'_4 | A'_5 | A'_6 |
|-----------------|--------|--------|--------|--------|--------|--------|--------|
| 0 | 1 | 0.47 | 0.93 | 0.29 | -0.32 | -0.33 | -0.29 |
| 350 | 1 | 0.26 | 0.68 | 0.23 | -0.18 | -0.25 | -0.18 |
| 500 | 1 | 0.21 | 0.65 | 0.18 | -0.17 | -0.13 | -0.11 |
| 1000 | 1 | 0.01 | 0.53 | 0.05 | -0.15 | -0.03 | -0.06 |
| 10000 | 1 | -0.01 | 0.59 | -0.01 | -0.15 | 0.00 | -0.05 |

Scattering of the ejected electron from this nonspherical potential can produce a larger contribution of odd and higher order electron partial waves than predicted for ionization of free NO(*C*). This scattering provides the opportunity for interference between odd and even partial waves, which causes the forward-backward asymmetry observed in this work. Similar asymmetry from intramolecular scattering has previously been observed in the inner shell ionization of CO [2] and autoionization of dissociating O₂ [15]. A combination of partial waves, including odd and higher order waves resulting from scattering, could also produce the lobed feature observed in the zero time delay PAD regardless of whether the NO₂ is linear or bent. Therefore, scattering of the photoelectron from the nonspherical potential created by the close proximity of the recoiling O atom to the NO⁺ provides the best single explanation for the zero time delay PAD features.

In the experiments with short time delays of 350 and 500 fs, ionization occurs when the dissociating O-NO bond is highly elongated so that the anisotropic scattering of the electron is weaker and the asymmetry observed in the PADs is less dramatic [Figs. 1(b) and 1(c)]. The changing asymmetry is quantitatively indicated by the decreasing magnitude of A'_K for odd K (Table I) as the time delay increases and the dissociation progresses. This constitutes the first observation of decreasing forward-backward asymmetry in PADs that results from increasing the molecular bond length. At long time delays of 1 and 10 ps, the dissociating bond is completely broken and the NO(*C*) rotates freely before being ionized by the probe laser pulse. This produces PADs that are symmetric and absent of lobed features at 30° [Figs. 1(d) and 1(e)]. The high degree of symmetry is also reflected by the negligible values of A'_K , for odd K , shown in Table I at long time delays. The A'_0 and A'_2 terms clearly dominate the fit, suggesting that the molecular sample is randomly oriented at long time delays, to a good approximation. Nonetheless, a small degree of angular momentum alignment [10] is indicated by the magnitude of the A'_4 term in Table I. For comparison with previous calculations of the asymmetry parameter, β , [see Eq. (1)], we have assumed a randomly oriented sample of NO(*C*) and determined a β value of 0.6 ± 0.1 , in good agreement with the calculated value of approximately 0.7 [14]. Hence, at time delays of 1 ps and longer, the PAD is produced by ionization of free NO(*C*), indicating that dissociation is complete.

In summary, this Letter presents femtosecond time-resolved PADs measured in the molecular frame of a dissociating molecule. Strong forward-backward asymmetry and a lobe at 30° from the O-NO dissociation axis are observed in the PADs at short time delays. These features are primarily attributed to scattering of the ejected electron from the highly nonspherical potential created by the close proximity of the O and NO fragments when ionization

occurs to yield NO⁺. As the dissociation proceeds, the PAD features rapidly evolve as the effect of the departing O atom on the ionization weakens. After 1 ps, the dissociation is complete and the PADs correspond to ionization of free NO(*C*). These unique experimental PADs for a dissociating molecule will provide an excellent test for recent theoretical treatments of photoelectron angular distributions [6,7,16,17].

We thank Mike Gutzler for his outstanding technical assistance. This work is supported by the U.S. Department of Energy, Office of Basic Energy Sciences, Division of Chemical Sciences.

*Permanent address: Department of Chemistry and Biochemistry, University of California–San Diego, 9500 Gilman Drive, La Jolla, CA 92093-0314.

†Corresponding author.

Email address: cchayde@sandia.gov

- [1] E. Shigemasa, J. Adachi, M. Oura, and A. Yagishita, Phys. Rev. Lett. **74**, 359 (1995); P. A. Hatherly, J. Adachi, E. Shigemasa, and A. Yagishita, J. Phys. B **28**, 2643 (1995); N. Watanabe *et al.*, Phys. Rev. Lett. **78**, 4910 (1997); E. Shigemasa *et al.*, Phys. Rev. Lett. **80**, 1622 (1998).
- [2] F. Heiser *et al.*, Phys. Rev. Lett. **79**, 2435 (1997).
- [3] A. V. Golovin, Opt. Spectrosc. **71**, 537 (1991); A. V. Golovin, N. A. Cherepkov, and V. V. Kuznetsov, Z. Phys. D **24**, 371 (1992).
- [4] P. Downie and I. Powis, Phys. Rev. Lett. **82**, 2864 (1999).
- [5] R. Dörner *et al.*, Phys. Rev. Lett. **81**, 5776 (1998).
- [6] Y. Arasaki, K. Takatsuka, K. Wang, and V. McKoy, Chem. Phys. Lett. **302**, 363 (1999); J. Chem. Phys. **112**, 8871 (2000).
- [7] S. C. Althorpe and T. Seideman, J. Chem. Phys. **110**, 147 (1999).
- [8] T. Zuo, A. D. Bandrauk, and P. B. Corkum, Chem. Phys. Lett. **259**, 313 (1996).
- [9] D. Dill, J. Chem. Phys. **65**, 1130 (1976).
- [10] S. W. Allendorf, D. J. Leahy, D. C. Jacobs, and R. N. Zare, J. Chem. Phys. **91**, 2216 (1989); D. J. Leahy, K. L. Reid, and R. N. Zare, J. Phys. Chem. **95**, 1757 (1991); K. L. Reid, D. J. Leahy, and R. N. Zare, Phys. Rev. Lett. **68**, 3527 (1992).
- [11] J. A. Davies, J. E. LeClaire, R. E. Continetti, and C. C. Hayden, J. Chem. Phys. **111**, 1 (1999).
- [12] J. V. Vallerga *et al.*, IEEE Trans. Nucl. Sci. **36**, 881 (1989).
- [13] J. W. Davenport, Phys. Rev. Lett. **36**, 945 (1976).
- [14] K. Wang, V. McKoy, and H. Rudolph, Chem. Phys. Lett. **216**, 490 (1994).
- [15] A. V. Golovin *et al.*, Phys. Rev. Lett. **79**, 4554 (1997).
- [16] I. Powis, Chem. Phys. **201**, 189 (1995); J. Chem. Phys. **106**, 5013 (1997).
- [17] J. G. Underwood and K. L. Reid, J. Chem. Phys. (to be published).